V. G. Lebedev[a], E. V. Abramova[a], D. A. Danilov[b], P. K. Galenko[c,d]

[a]Faculty of Physics and Energetics, Udmurt State University, Izhevsk, Russia
[b]Theoretical Biophysics Group, Karlsruhe Institute of Technology (KIT), Karlsruhe, Germany
[c]Institut für Materialphysik im Weltraum, Deutsches Zentrum für Luft- und Raumfahrt (DLR), Köln, Germany
[d]Institut für Festkörperphysik, Ruhr-Universität Bochum, Bochum, Germany

Phase-field modeling of solute trapping: comparative analysis of parabolic and hyperbolic models

The phase-field model of Wheeler, Boettinger and McFadden is extended to the case of fast solidification in which local non-equilibrium phenomena occur in the bulk phases and within the diffuse solid – liquid interface. Such an extension leads to the characteristic diffusion speeds of atoms (both within the diffuse interface and inside the bulk phases) and to the speed of the interface propagation. As a result, the model is described by a system of hyperbolic equations for the atomic diffusion transport as well as for the phase-field. This model is applied to the problem of solute trapping, which is accompanied by the entrapment of solute atoms beyond chemical equilibrium by a rapidly moving interface. The model predicts the beginning of complete solute trapping and diffusionless solidification at a finite solidification velocity.

Keywords: Phase-field; Solute trapping; Rapid solidification

1. Introduction

The term "solute trapping" has been introduced to describe the process of non-equilibrium solute redistribution at the solid – liquid interface, which is accompanied by the entrapment of solute away from chemical equilibrium in solidification [1, 2]. This process results in the deviation of the partition coefficient for solute distribution at the interface towards unity away from its equilibrium value, independently of the sign of the chemical potential [3, 4].

Valuable advancements were made previously by Aziz et al. [3 – 6] in describing nonequilibrium solute redistribution at the rapidly moving solid – liquid interface during the solidification of binary melts. The nonequilibrium solute redistribution is characterized by the solute segregation coefficient $k(V)$, which is dependent on the interface velocity V, and is evaluated by the following ratio

$$k(V)_{\text{interface}} = \frac{\text{concentration in solid}}{\text{concentration in liquid}} \qquad (1)$$

This segregation coefficient $k(V)$ includes the kinetic parameter in a form of the solute diffusion speed V_{DI} at the interface [3 – 6]. Quantitative analysis of such a function $k(V)$ shows reasonable agreement with experimental findings [7] at small and moderate growth velocities of crystals (see discussion in Ref. [8]). Many attempts have also been made to describe solute trapping during rapid solidification using phase-field model [9 – 14]. As a result of these investigations, the segregation coefficient $k(V)$ is found to increase monotonically and gradually as the velocity V increases (see, e.g., Ref. [14]), following the predictions of the continuous growth model [3, 4]. However, in contrast to the results of natural experiments [2, 15 – 23] as well as to predictions of molecular dynamic simulations [24], numerical predictions based on the phase-field models [9 – 14] were not able to reach the complete solute trapping regime which occurs at $k(V) = 1$ (see, for overview, Ref. [25]). These model solutions are obtained for the parabolic type of diffusion equation (which assumes infinite speed for atomic bulk diffusion), with the only diffusion speed being V_{DI}, i. e. the diffusion speed within the diffuse interface. Therefore, to describe increasing $k(V)$ up to $k(V) = 1$ at a finite V, one can suggest extending the model by introducing the finite speed of atomic diffusion in bulk phases. The main scope of the present article is to develop such a phase-field model which takes into account both solute diffusion speeds within the diffuse interface and bulk phases. This development is given in a form of extended Wheeler – Boettinger – McFadden phase-field model (the WBM-model) [9], previously adopted by Ahmad et al. [12] to the problem of solute trapping. Such extension leads to a model represented by a couple of partial differential equations of hyperbolic type. To predict the complete solute trapping observable in experiments and predicted by the sharp-interface model (see results and discussion in Ref. [26]), the fully hyperbolic model is analyzed, and the results compared with those of the parabolic phase-field model [9, 12].

2. The model

To describe the evolution of the concentration C and the phase-field variable φ in an isothermal system at constant temperature T, the following functional of the free energy is used [27]

$$F = \int_{\Omega} \left(f(C, \varphi, \boldsymbol{J}, \dot{\varphi}) + \frac{1}{2} \varepsilon_{\varphi}^2 |\nabla \varphi|^2 \right) \mathrm{d}\Omega \qquad (2)$$

where $\boldsymbol{J}$ is the atomic diffusion flux, $\dot{\varphi} \equiv \partial\varphi/\partial t$ the rate of change of the phase field, t the time, Ω the volume of the system, and ε_φ a quantity proportional to the correlation length of the phase field. The term $|\nabla\varphi|^2$ appears as in the gradient theories of van der Vaals and Ginzburg–Landau types. The free energy density $f(C, \varphi, \boldsymbol{J}, \dot{\varphi})$ is defined as the additive sum of an equilibrium part f_e and a non-equilibrium contribution f_ne, such that

$$f(C, \varphi, \boldsymbol{J}, \dot{\varphi}) = f_\mathrm{e}(C, \varphi) + f_\mathrm{ne}(\boldsymbol{J}, \dot{\varphi}) \tag{3}$$

2.1. Local non-equilibrium contribution to the free energy density

The pure non-equilibrium contribution f_ne in Eq. (3) takes into account the relaxation of $\boldsymbol{J}$ to its steady state and the rate of change of the phase field $\dot{\varphi}$. In the first approximation

$$f_\mathrm{ne}(\boldsymbol{J}, \dot{\varphi}) = \frac{\alpha_J}{2} J^2 + \frac{\alpha_\varphi}{2} \dot{\varphi}^2 \tag{4}$$

where α_J and α_φ are phenomenological coefficients proportional to the relaxation time τ_D of $\boldsymbol{J}$ and the time τ_φ for the relaxation of $\dot{\varphi}$. The contribution (4) to the free energy is considered as a kinetic contribution to the fast solidification (in a manner of results summarized in Ref. [28]). In the limit of the instant relaxation of $\boldsymbol{J}$ and $\dot{\varphi}$ the local non-equilibrium contribution to the free energy density disappears, i.e., $f_\mathrm{ne}(\boldsymbol{J}, \dot{\varphi}) \to 0$. In this case, Eq. (3) defines the free energy density as $f_\mathrm{e}(C, \varphi)$ for the local equilibrium binary system [12].

For the functional (2), the requirement that the free energy monotonically decreases ($\mathrm{d}F/\mathrm{d}t < 0$) during the relaxation of the entire system to equilibrium leads to the following equations

$$\tau_\mathrm{D}\ddot{C} + \dot{C} = \nabla \cdot \left[M_C \left(f_{CC}\nabla C + f_{C\varphi}\nabla\varphi \right) \right] \tag{5}$$

$$\tau_\varphi\ddot{\varphi} + \dot{\varphi} = M_\varphi(\varepsilon_\varphi^2 \Delta\varphi - f_\varphi) \tag{6}$$

where τ_D is the relaxation time for the diffusion flux, M_C the mobility of B-atoms, τ_φ the time scale for the relaxation of the rate of change of the phase field $\dot{\varphi}$, and M_φ is the mobility of the phase field. Also, the following notation for derivatives are accepted: $\dot{C} \equiv \partial C/\partial t$, $\ddot{C} \equiv \partial^2 C/\partial t^2$, $f_C \equiv \partial f/\partial C$, $f_{C\varphi} \equiv \partial^2 f/\partial C\partial\varphi$, $f_{CC} \equiv \partial^2 f/\partial C^2$, $\ddot{\varphi} \equiv \partial^2\varphi/\partial t^2$, $f_\varphi \equiv \partial f/\partial\varphi$. Eqs. (5) and (6) represent a fully hyperbolic system in which the free energy does not increase in time and the atomic balance law is satisfied with the assumption of positivity of the mobility coefficients [27].

2.2. Local equilibrium contribution to the free energy density

To complete the definition of the system (5) and (6), let us choose the concrete free energy density f_e under condition of local equilibrium. Following the WBM-model [12], the local equilibrium free energy density f_e is chosen as the ideal solution of a binary system:

$$f_\mathrm{e}(C, T, \varphi) = (1 - C) f_\mathrm{A}(T, \varphi) + C f_\mathrm{B}(T, \varphi) \tag{7}$$

$$+ \frac{RT}{v_\mathrm{m}} \left((1 - C)\ln(1 - C) + C\ln C \right) + Wg(\varphi)$$

where R is the gas constant, v_m the molar volume (constant for A- and B-atoms), W the height of the energetic barrier which is modeled by the double-well function

$$g(\varphi) = \varphi^2(1 - \varphi)^2 \tag{8}$$

The energy densities $f_\mathrm{A}(T, \varphi)$ and $f_\mathrm{B}(T, \varphi)$ of A and B atoms, respectively, are derived using the dilute alloy approximation (see Appendix A)

$$f_\mathrm{A}(T, \varphi) = \frac{RT}{v_\mathrm{m}} F_\mathrm{A}(T) (1 - p(\varphi)) \tag{9}$$

$$F_\mathrm{A}(T) = \ln \frac{1 + (1/m_\mathrm{e})(T_\mathrm{A} - T)}{1 + (k_\mathrm{e}/m_\mathrm{e})(T_\mathrm{A} - T)}$$

$$f_\mathrm{B}(T, \varphi) = \frac{RT}{v_\mathrm{m}} F_\mathrm{B}(T) (1 - p(\varphi)), \quad F_\mathrm{B} = -\ln k_\mathrm{e} \tag{10}$$

Using a common tangent construction (see, e. g., Ref. [10]), this approximation leads to straight lines of the solidus $T_\mathrm{S} = T_\mathrm{A} + m_\mathrm{e}C/k_\mathrm{e}$ and the liquidus $T_\mathrm{L} = T_\mathrm{A} + m_\mathrm{e}C$ in the phase diagram with the equilibrium coefficient k_e for the B-atom partitioning and the tangent m_e of the liquidus line. The interpolation function $p(\varphi)$ is taken to be

$$p(\varphi) = 30 \int_0^\varphi g(s)\,\mathrm{d}s = 6\varphi^5 - 15\varphi^4 + 10\varphi^3 \tag{11}$$

with

$$1 - p(\varphi) = p(1 - \varphi), \quad p'(0) = p'(1) = p''(0) = p''(1) = 0 \tag{12}$$

The functions $g(\varphi)$ and $p(\varphi)$ (given by Eqs. (8) and (11), respectively) are a feature of the specific choice of phase-field model used here, which is described in Wang et al. [29]. As a result of adaptation to an alloy [30], these functions define the liquid state for $\varphi = 1$ and the solid state for $\varphi = 0$.

3. Numerical solution

3.1. Parameters of the phase field and solute diffusion

The present computations use the model parameters introduced in Refs. [9, 12, 30]. These are:
– the gradient energy factor ε_φ^2, the energetic barrier height W, the capillary parameter d_0, and the mobility M_φ of the phase field expressed in terms of the surface energy σ, the interfacial width δ, and the field diffusion parameter v:

$$\varepsilon_\varphi^2 = 2\sigma\delta, \quad W = \frac{9\sigma}{\delta}, \quad d_0 = \frac{\sigma v_\mathrm{m}}{RT_\mathrm{A}}, \quad M_\varphi = \frac{v}{2\sigma\delta} \tag{13}$$

– the diffusion coefficient of B-atoms (in the accepted dilute alloy approximation) within the diffuse interface taking into account bulk diffusion coefficients D_L and D_S in the liquid and solid, respectively:

$$D(\varphi) = D_\mathrm{S} + p(\varphi)(D_\mathrm{L} - D_\mathrm{S}) \tag{14}$$

– the atomic mobility:

$$M_C(T, C, \varphi) = \frac{D(\varphi)}{f_{CC}(T, C, \varphi)} \tag{15}$$

Note that the atomic mobility (15) is positive at $f_{CC} > 0$. Also, to guarantee monotonic behavior of the free energy and to give non-positive dissipation of the free energy in the solidifying system, the phase field mobility from Eq. (13) is also assumed to be positive.

3.2. Equations in the moving reference frame

The solute trapping problem is analyzed in one spatial dimension with a planar interface using the model parameters (13)–(15). In this case, we use the following dimensionless co-ordinate reference frame, $x \to (x - Vt)/\delta$ and $t \to tv/\delta^2$, which is moving with the constant interface velocity V with the origin $x = 0$ placed at $\varphi = 1/2$. Then, the governing equations (5) and (6) can be written in the following dimensionless form:

– the concentration field

$$\frac{V^2}{(V_D^B)^2} \frac{\partial^2 C}{\partial x^2} - \frac{V}{V_D^I} \frac{\partial C}{\partial x} = \frac{\partial}{\partial x}\left(\hat{D}(\varphi)\frac{\partial C}{\partial x}\right)$$

$$+ \Theta(T) \frac{\partial}{\partial x}\left(\hat{D}(\varphi)C(1 - C)\frac{\partial p(\varphi)}{\partial \varphi}\frac{\partial \varphi}{\partial x}\right) \quad (16)$$

– the phase field

$$\frac{V^2}{(V_\varphi^B)^2} \frac{\partial^2 \varphi}{\partial x^2} - \frac{V}{V_\varphi^I} \frac{\partial \varphi}{\partial x} = \frac{\partial^2 \varphi}{\partial x^2} - \frac{9}{2}\frac{\partial g}{\partial \varphi}$$

$$+ \frac{1}{2}\frac{\delta}{d_0}\frac{T}{T_A}\Lambda(T, C)\frac{\partial p(\varphi)}{\partial \varphi} \quad (17)$$

Equations (16) and (17) describe quasi-stationary phase-field dynamics in which, using contributions to the free energy density given in Subsection 2.2, the following functions are introduced

$$\Theta(T) = \ln\left(\frac{1 + (1/m_e)(T_A - T)}{1 + (k_e/m_e)(T_A - T)}\right) + \ln k_e \quad (18)$$

$$\Lambda(T, C) = (1 - C)\ln\left(\frac{1 + (1/m_e)(T_A - T)}{1 + (k_e/m_e)(T_A - T)}\right) - C\ln k_e$$

$$(19)$$

and, using the definition (14), the dimensionless diffusion coefficient is

$$\hat{D}(\varphi) = D(\varphi)/D_L = D_S/D_L + p(\varphi)(1 - D_S/D_L) \quad (20)$$

Equations (16) and (17) include the following interfacial and bulk characteristic speeds: V_D^I the diffusion speed within the diffuse interface, V_φ^I the speed for phase field propagation within the interface, V_D^B the diffusion speed in the bulk liquid, and V_φ^B the speed for propagation of the phase field into the bulk phases. Using the analytical expressions for these characteristic speeds from Table 1, within the local equilibrium limits $\tau_D \to 0$ and $\tau_\varphi \to 0$, the bulk speeds become infinite $V_D^B \to \infty$ and $V_\varphi^B \to \infty$. In this case, the system (16) and (17) transforms into the previously investigated case of solute trapping [12, 14] which takes into account local non-equilibrium effects within the diffuse interface only.

Table 1. Analytical expressions for the characteristic speeds of the atomic diffusion and the phase field propagation.

Parameter	Expression
Speed of solute diffusion within the diffuse interface	$V_D^I = D_L/\delta$
Speed for phase field propagation within the interface	$V_\varphi^I = v/\delta$
Speed of solute diffusion in bulk liquid	$V_D^B = (D_L/\tau_D)^{1/2}$
Speed for phase field propagation into bulk phases	$V_\varphi^B = (v/\tau_\varphi)^{1/2}$

3.3. Methods of solution

The numerical solution is obtained for the specific case of a Si-9 at.% As alloy with material parameters given in Table 2 (see also data from Refs. [31] and [32]). Taking the first integral from Eq. (16), we arrive at the following equation for solute diffusion

$$\bar{D}(\varphi)\frac{dC}{dx} + \Theta(T)\hat{D}(\varphi)C(1 - C)\frac{\partial p(\varphi)}{\partial \varphi}\frac{\partial \varphi}{\partial x} + \frac{V}{V_D^I}(C - C_0) = 0 \quad (21)$$

In this equation, the dimensionless diffusion parameter

$$\bar{D}(\varphi) = (\hat{D}(\varphi) - (V/V_D^B)^2)\,\theta[\hat{D}(\varphi) - (V/V_D^B)^2] \quad (22)$$

is introduced with the Heaviside function

$$\theta[r] = \begin{cases} 1, & r > 0 \\ 0, & r \leq 0 \end{cases} \quad (23)$$

The definition of parameter (22) takes into account the extremely fast propagation of the interface when $\hat{D}(\varphi) - (V/V_D^B)^2 < 0$. The latter inequality leads to the diffusion field instability and abnormal increase of computed values for concentrations which have no physical meaning. Physically this instability leads to the fact that diffusion has no time to act in the rapidly crystallizing local bulk of the system in which the interface velocity V is equal or greater than the diffusion speed V_D^B in bulk liquid. Therefore, instead of the difference $\hat{D}(\varphi) - (V/V_D^B)^2$ appearing after the first integration of Eq. (16), we introduce the diffusion parameter (22) which exhibits suppression of the atomic diffusion when $\hat{D}(\varphi) - (V/V_D^B)^2 < 0$.

Table 2. Physical parameters of the Si-9 at.% As alloy used for the phase-field modeling.

Parameter	Value	Reference
T_A	1 685 K	[31]
m_e	-400 K/at. frac.	[14]
k_e	0.3	[7, 32]
v_m	$1.2 \cdot 10^{-5}$ m³/mol⁻¹	[14]
D_L	$1.5 \cdot 10^{-9}$ m² s⁻¹	[32]
D_S	$3 \cdot 10^{-13}$ m² s⁻¹	[32]
σ	0.477 m²	[31]
v	$1.22 \cdot 10^{-8}$ m² s⁻¹	[14]
δ	$1.875 \cdot 10^{-9}$ m	present work
τ_φ	$1.0 \cdot 10^{-11}$ s	present work
τ_D	$3.4 \cdot 10^{-10}$ s	from Table 1
$V_\varphi^I = v/\delta$	6.51 m s⁻¹	from Table 1
$V_\varphi^B = (v/\tau_\varphi)^{1/2}$	34.9 m s⁻¹	from Table 1
$V_D^I = D_L/\delta$	0.8 m s⁻¹	[25]
$V_D^B = (D_L/\tau_D)^{1/2}$	2.1 m s⁻¹	[25]

Equations (21)–(23) are solved numerically by the Runge–Kutta method simultaneously with the phase-field Eq. (17) resolved by the relaxation method as follows:

$$\frac{\partial \varphi}{\partial \eta} = [1 - (V/V_\varphi^B)^2] \frac{\partial^2 \varphi}{\partial x^2} + \frac{V}{V_\varphi^I} \frac{\partial \varphi}{\partial x}$$
$$- \frac{\partial}{\partial \varphi} \left(\frac{9}{2} g(\varphi) - \frac{1}{2} \frac{\delta}{d_0} \frac{T}{T_A} \Lambda(T,C) \, p(\varphi) \right) \qquad (24)$$

Here η is the effective "relaxation time".

The origin $x_0 = 0$ of the moving reference frame is placed in the point $\varphi = 1/2$ of the diffuse interface, therefore, the temperature T is relaxed by

$$\frac{1}{T_A} \frac{\partial T}{\partial \eta} = \frac{1}{\eta_V} \frac{\partial x_0}{\partial \eta} + \frac{1}{\eta_X} x_0 \qquad (25)$$

Here η_V and η_X are numeric parameters of relaxation. The first term on the right hand side of Eq. (25) gives a feedback from the temperature to the relative interface velocity in the moving reference frame to reach $\partial x_0 / \partial \eta \to 0$. The second term on the right hand side of Eq. (25) "attracts" the moving interface to the point $\varphi = 1/2$ providing $x_0 \to 0$. In limiting cases $\partial \varphi / \partial \eta \to 0$ and $\partial T / \partial \eta \to 0$, one obtains the stationary profiles of $\varphi(x)$ and $C(x)$ in the moving reference frame.

Relaxation parameters η_V and η_X are used for optimizing the relaxation process. For a given interface velocity V, the relaxation takes about $10^5 - 10^3$ iterations with the step $d\eta \approx 0.01$ of the "relaxation time" depending on the initial approximation and the value of V.

3.4. Initial and boundary conditions

The initial condition for φ is taken as the diffuse step function $\varphi = 0.5[1 + \tanh\{3x/(2\delta)\}]$ and the temperature as $T < T_A$. Boundary conditions for the phase field are

$$\varphi(\infty) = 1, \quad \varphi(-\infty) = 0 \qquad (26)$$

Because Eq. (21) is a first order differential equation, it does not require specific boundary conditions for the concentration field. Therefore, we found the solution of Eqs. (21)–(23) for $\bar{D}(\varphi) > 0$ within the Cauchy problem. The following three cases are specified in the numerical solution.

(i) Let $(V/V_D^B)^2 < D_S/D_L$. Then, Eqs. (20) and (22) give $\bar{D}(\varphi) > 0$ for any x. Equation (21) is easily integrated far from the interface with $\partial p(\varphi(x))/\partial x \to 0$ to give the following solution

$$C(x) = C_0 + A \exp(-\alpha x) \quad \text{for} \quad \alpha > 0$$

Assuming that $C(x)$ is finite as $x \to -\infty$ one finds $C(x) = C_0$ at $\varphi = 0$. Thus, together with the initial condition $C|_{\varphi=0} = C_0$, Eq. (21) defines the Cauchy problem and a profile of concentration for any x.

In the case of a very small value of $\bar{D}$, Eq. (21) is integrated numerically in the following parametrical form

$$\begin{cases} \dfrac{dx}{ds} = \bar{D}(\varphi(x(s))) \\ \dfrac{dC}{ds} = -\Theta(T) D(\varphi) C(x)(1 - C(x)) \dfrac{dp(\varphi(x))}{dx} - \dfrac{V}{V_D^I}(C - C_0) \end{cases} \qquad (27)$$

where s is some formal parameter.

(ii) Let $V/V_D^B > 1$. Then, Eqs. (20) and (22) give $\bar{D}(\varphi) \equiv 0$ for any x. Equation (21) is reduced to a quadratic equation for $C(x)$ with solution $C(x) = C_0$ when $\partial p(\varphi(x))/\partial x \to 0$. If $\partial p(\varphi(x))/\partial x \neq 0$, the physically meaningful root has a value between 0 and 1 and is smoothly as with $C = C_0$ at $\partial p/\partial x = 0$. This root determines the profile for $C(x)$.

(iii) In the intermediate case, $D_S/D_L \leq (V/V_D^B)^2 \leq 1$, one finds $\bar{D}(\varphi) \equiv 0$ in some region $x \leq x_c$, where $C(x)$ is again defined by the quadratic equation discussed in (ii). To obtain the initial condition for $C(x)$ in the region $x > x_c$, one can integrate Eq. (16) in a small ε-vicinity of a point x_c:

$$\bar{D}(\varphi(x_c + \varepsilon)) \frac{\partial C}{\partial x}\bigg|_{x=x_c+\varepsilon} + (V/V_D^I)(C(x_c + \varepsilon) - C(x_c - \varepsilon))$$

$$+ \Theta(T) D(\varphi(x)) C(x)(1 - C(x)) \frac{\partial p(\varphi(x))}{\partial x}\bigg|_{x_c-\varepsilon}^{x_c+\varepsilon} = 0 \qquad (28)$$

Representing the derivative $(\partial C/\partial x)|_{x=x_c+\varepsilon}$ by $[C(x_c + \varepsilon) - C(x_c)]/\varepsilon$ and substituting it in Eq. (28), one finds the initial condition for the Cauchy problem in $x > x_c$.

4. Results of the modeling

We consider the specific case of a Si-9 at.% As alloy with material parameters from Table 2. Numerical solutions for the parabolic WMB-model [9, 12, 14] are obtained by solving Eqs. (21), (24), and (25) [together with Eqs. (14), (18)–(20)] with the local equilibrium limits $V_D^B \to \infty$ and $V_\varphi^B \to \infty$. The fully hyperbolic extension of the WBM-model is given by the governing equations (21) and (24) (using Eqs. (18)–(20)), the diffusion parameters (22) and (23), the temperature relaxation term (25), and the conditions of Section 3.4. The predictions of the parabolic WBM-model and its hyperbolic extension are compared for the obtained results of concentration fields (Fig. 1), the solute trapping by the solute segregation coefficient on a diffuse interface (Fig. 2), the "velocity–temperature" relationship (Fig.3), and the kinetic phase diagrams (Fig. 4).

5. Discussion

5.1. Concentration profiles

The change in the concentration profile (for atoms of As considered as a solute in the Si-9 at.% As alloy) as the interface velocity increases is shown in Fig. 1. It is seen that, as the velocity increases, the width of concentration profile of the present hyperbolic extension of the WBM-model shrinks faster than the parabolic WBM-model. With the higher interface velocity, the small "hill" of the concentration profile is localized within the diffuse interface of the hyperbolic model (see profile at $V = 2.8 \text{ m s}^{-1}$). Note that the position of the solute diffusion profiles at a given velocity depends on the chosen interfacial width δ. This dependence could be a subject of future modeling.

5.2. Solute segregation

In the context of a diffuse-interface description, solute segregation has been defined as the ratio of concentrations in the solid and at the maximum of concentration profile

476

[12]. This definition has been analyzed and revised (see discussion in Ref. [14]). In particular, it has been suggested to take the ratio of concentrations at some distance from the "center" of the diffuse interface, which belongs to the solid and liquid phases from both sides of the interface. In the present work, to evaluate numerically the solute segregation coefficient (1), we take the definition $k(V) = (C|_{\varphi=0.001})/(C|_{\varphi=0.999})$, which is consistent, in principle, with the one given in Ref. [14]. Therefore, using the computed concentrations, in Fig. 1, the solute segregation coefficient is computed as a function of interface velocity V at the values of $\varphi = 0.001$ for the solid and $\varphi = 0.999$ for the liquid phase, which actually establish the boundaries of the diffuse interface.

As is shown in Fig. 2, the parabolic WBM-model predicts a gradual increase of the non-equilibrium solute segregation coefficient $k(V)$ in the entire region of the interface velocity V investigated. These results reproduce previous predictions obtained by the WBM-type model [12, 14]. By contrast, the hyperbolic model predicts a more abrupt change to the complete solute trapping, $k(V) \equiv 1$, at a fixed interface 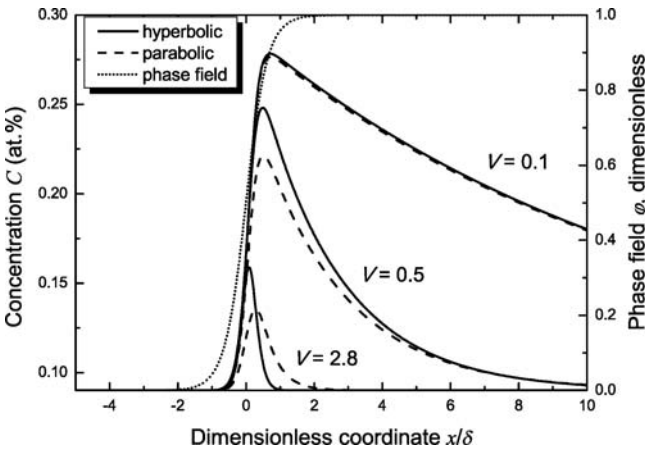velocity as is clearly seen in Fig. 2. This result is qualitatively consistent with experimental findings [2, 15–23], results of molecular dynamic simulations [24], and outcomes from the hyperbolic extension of the continuum growth model [25].

5.3. Temperature and interface velocity

The temperature T as a function of the interface velocity V differs substantially between both models. The gradual shrinking of the concentration profile and the gradual increase in the solute trapping function predicted by the parabolic WBM-model (see Figs. 1 and 2) leads to a smooth and gradual behavior of the $T(V)$-function (see upper curves in Fig. 3). In contrast, the hyperbolic WBM-model predicts non-monotonic behavior of the $T(V)$-function with a clear minimum in temperature at some value of the velocity. The minimum in the $T(V)$-function is consistent with the drastic shrinking of the solute diffusion profile up to the

Fig. 3. Dependence of temperature in the computational domain on interface velocity. Results for the parabolic WBM-model and its extension to the hyperbolic model are shown for various solid–liquid interface widths δ in solidifying Si-9 at.% As alloy.

Fig. 1. Concentration profiles for different interface velocities (indicated as "V" with dimensionality "m s^{-1}") and the phase-field profile. Calculations were carried out for Si-9 at.% As alloy and the constant interface width $\delta = 1.2 \cdot 10^{-9}$ m.
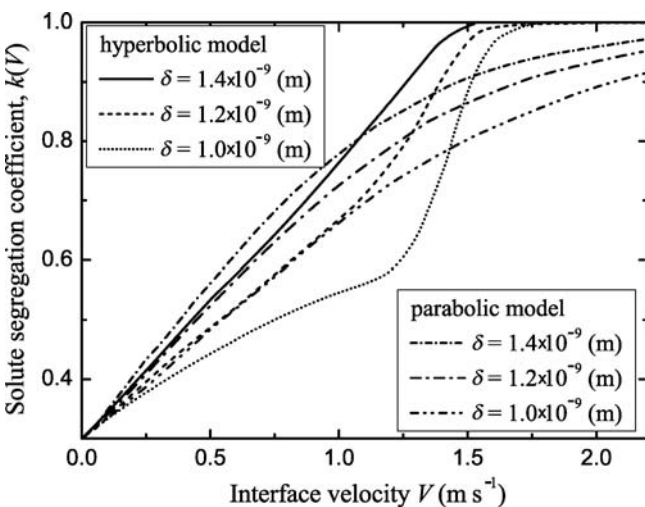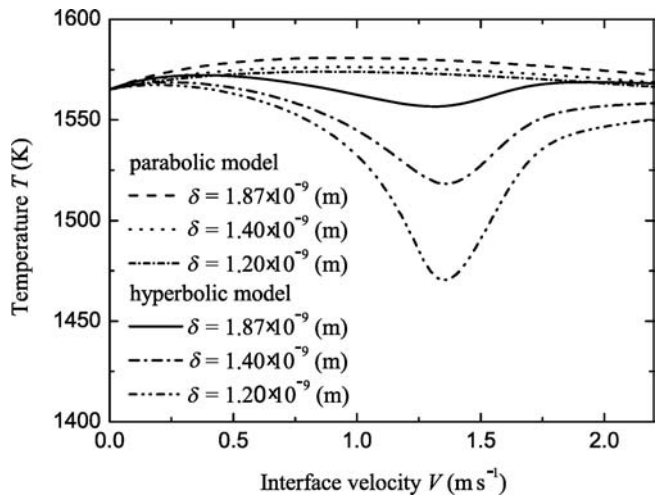

Fig. 2. Non-equilibrium solute segregation coefficient $k(V)$ for Si-9 at.% As alloy. Results of the modeling are summarized for the parabolic WBM-model, and its extension to the hyperbolic model, at various interfacial widths δ.
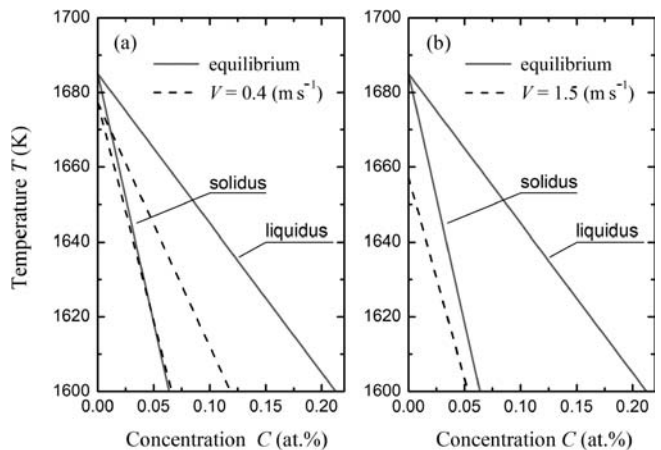

Fig. 4. Kinetic phase diagram with the linear approximation of liquidus and solidus lines for Si–As alloys derived from the hyperbolic model. Solid lines represent equilibrium lines of the liquidus and solidus. Dashed lines give kinetic liquidus and solidus. (a) Shift of the kinetic liquidus and solidus from their equilibrium positions at the interface velocity $V = 0.4$ (m s^{-1}). (b) Confluence of the kinetic liquidus and solidus in one line as a result of the complete solute trapping and diffusionless solidification. Computations are made for the interfacial width from Table 2.

characteristic length $L_D = 2D[1 - (V^2/V_D^B)^2]/V$ comparable with the interface width: $L_D \propto \delta$. Therefore, as predicted by the hyperbolic model (see the lower curves in Fig. 3), one can distinguish between:

– the regime with increasing undercooling to surmount the resistance of the developed solute atmosphere around the interface. This regime exists from the smallest interface velocity up to the interface velocity at which the $T(V)$-function is at minimum,
– the regime in which the system and, especially, the interface are heating up with a decrease in undercooling due to the absence of developed solute diffusion profile. This regime exists from the velocity giving the minimum of the $T(V)$-function up to highest velocity giving complete solute trapping.

5.4. Kinetic phase diagrams

Figure 4 exhibits kinetic phase diagrams of the rapid solidification of the alloy in the coordinates "interface temperature–concentration" constructed using modeling results of the hyperbolic extension of the WBM-model. We found that the actual interval of solidification, as a distance between lines of liquidus and solidus, shrinks with the increase in interface velocity V. This is clearly seen by comparing the solid lines for the equilibrium state with $V = 0$ (m s^{-1}) and the dashed lines for kinetic liquidus and solidus lines for $V = 0.4$ (m s^{-1}), shown in Fig. 4a. With a higher interface velocity, $V \geq 1.5$ (m s^{-1}), the kinetic liquidus and solidus lines merge into one line, shown as a dashed line in Fig. 4b. This result indicates the equality of the solid and liquid concentrations on both sides of the diffuse interface: in the modeling we found

$$C|_{\varphi=0.001} = C|_{\varphi=0.999}$$

$\equiv$ initial (nominal) alloy composition with $k(V) \equiv 1$.

This result can be recognized as one of the main characteristics of complete solute trapping that accompanies diffusionless solidification.

Note that using the parabolic system of phase-field equations one can find that kinetic liquidus and solidus lines only gradually approach each other as the velocity V increases (see, e.g., kinetic diagram in Fig. 4 of Ref. [13]). Chemically partitionless solidification is also predicted previously using a sharp-interface model in which solute transport has been described by the hyperbolic equation (see, e.g., kinetic diagram in Fig. 4 of Ref. [33]).

6. Conclusions

The phase-field parabolic model of Wheeler, Boettinger and McFadden (WBM-model) [9, 12] has been extended to the case of local non-equilibrium solidification. Four kinetic parameters were appearing in the model as main characteristics of local non-equilibrium effects. These are the characteristic speeds of atomic diffusion and phase field propagation within and around the moving diffuse solid–liquid interface (see Table 1). The model is described by a system of hyperbolic partial differential equations for the atomic diffusion transport and diffuse interface advance-

ment. The present model is applied to the solute trapping problem. Modeling results have been analyzed by considering solute concentration profiles, the solute segregation coefficient, "temperature–velocity" relationships, and kinetic phase diagrams. A comparison with the predictions of the parabolic WBM-model has shown that the present hyperbolic extension of WBM-model predicts that complete solute trapping and diffusionless solidification begin at the fixed interface velocity. At this critical point, the alloy solidifies as a supersaturated solid solution with the initial chemical composition. Finally, to compare modeling predictions with experimental data, the model can be generalized to the non-ideal solution and concentrated binary system.

References

[1] A.A. Chernov, in: A.V. Shubnikov, N.N. Sheftal (Eds.), Rost Kristallov Vol. 3, Akademia Nauk SSSR, Moscow, (1959) [English translation: Growth of Crystals, Vol. 3, Consultants Buro, New York (1962) p. 35].
[2] J.C. Baker, J.W. Cahn: Acta Metall. 17 (1969) 575. DOI:10.1016/0001-6160(69)90116-3
[3] M.J. Aziz: J. Appl. Phys. 53 (1982) 1158. DOI:10.1063/1.329867
[4] M.J. Aziz, T. Kaplan: Acta Metall. 36 (1988) 2335. DOI:10.1016/0001-6160(88)90333-1
[5] M.J. Aziz, W.J. Boettinger: Acta Metall. Mater. 42 (1994) 527. DOI:10.1016/0956-7151(94)90507-X
[6] M.J. Aziz: Metall. Mater. Trans A 27 (1996) 671. DOI:10.1007/BF02648954
[7] J.A. Kittl, P.G. Sanders, M.J. Aziz, D.P. Brunco, M.O. Thompson: Acta Mater. 48 (2000) 4797. DOI:10.1016/S1359-6454(00)00276-7
[8] P. Galenko: Mater. Sci. Eng. A 375 (2004) 493. DOI:10.1016/j.msea.2003.10.013
[9] A.A. Wheeler, W.J. Boettinger, G.B. McFadden: Phys. Rev. E 47 (1993) 1893. DOI:10.1103/PhysRevE.47.1893
[10] W.J. Boettinger, A.A. Wheeler, B.T. Murray, G.B. McFadden: Mater. Sci. Eng. A 178 (1994) 217. DOI:10.1016/0921-5093(94)90546-0
[11] M. Conti: Phys. Rev. E 56 (1997) 3717. DOI:10.1103/PhysRevE.56.3717
[12] N.A. Ahmad, A.A. Wheeler, W.J. Boettinger, G.B. McFadden: Phys. Rev. E 58 (1998) 3436. DOI:10.1103/PhysRevE.58.3436
[13] K. Glasner: Physica D 151 (2001) 253. DOI:10.1016/S0167-2789(01)00231-7
[14] D. Danilov, B. Nestler: Acta Mater. 54 (2006) 4659. DOI:10.1016/j.actamat.2006.05.045
[15] W.T. Olsen, R. Hultgren: Trans. AIME 188 (1950) 1323.
[16] P. Duwez, R.H. Willens, W. Klement (Jr.): J. Appl. Phys. 31 (1960) 1136. DOI:10.1063/1.1735777
[17] D.S. Kamenetskaya, E.P. Rakhmanova, Y.S. Spektor: Sov. Phys.-Dokl. 7 (1962) 72.
[18] H. Biloni, B. Chalmers: Transactions AIME 233 (1965) 373.
[19] H. Jones: Rep. Prog. Phys. 36 (1973) 1425. DOI:10.1088/0034-4885/36/11/002
[20] I.S. Miroshnichenko: Quenching From the Liquid State, Metallurgia, Moscow (1982).
[21] N. Jacobson: Mater. Sci. Eng. A 133 (1991) 574. DOI:10.1016/0921-5093(91)90137-C
[22] S.C. Sharma, D.M. Herlach: Microgravity Science Technol. 3 (1992) 145.

[23] F.M. Costa, M.F. Carrasco, R.F. Silva, J.M. Vieira: Supercond. Sci. Technol. 16 (2003) 392. DOI:10.1088/0953-2048/16/3/311
[24] S.J. Cook, P. Clancy: J. Chem. Phys. 99 (1993) 2175. DOI:10.1063/1.465280
[25] P. Galenko: Phys. Rev. E 76 (2007) 031606. DOI:10.1103/PhysRevE.76.031606
[26] P.K. Galenko, D.M. Herlach: Phys. Rev. Lett. 96 (2006) 150602. DOI:10.1103/PhysRevLett.96.150602 PMid:16712141
[27] P. Galenko, D. Jou: Phys. Rev. E 71 (2005) 046125. DOI:10.1103/PhysRevE.71.046125
[28] P. Galenko, D. Jou: Physica A 388 (2009) 3113. DOI:10.1016/j.physa.2009.04.003
[29] S.-L. Wang, R.F. Sekerka, A.A. Wheeler, B.T. Murray, S.R. Coriell, R.J. Brown, G.B. McFadden: Physica D 69 (1993) 189. DOI:10.1016/0167-2789(93)90189-8
[30] J.A. Warren, W.J. Boettinger: Acta Mater. 43 (1995) 689. DOI:10.1016/0956-7151(94)00285-P
[31] B. Vinet, L. Magnusson, H. Fredriksson, P.J. Desre: J. Colloid Interface Science 255(2) (2002) 363. PMid:12505085; DOI:10.1006/jcis.2002.8627
[32] J.A. Kittl, M.J. Aziz, D.P. Brunco, M.O. Thompson: J. Cryst. Growth 148 (1995) 172. DOI:10.1016/0022-0248(94)00836-1
[33] P. Galenko, S. Sobolev: Phys. Rev. E 55 (1997) 343. DOI:10.1103/PhysRevE.55.343

Correspondence address

Peter Galenko
Institut für Materialphysik im Weltraum
Deutsches Zentrum für Luft- und Raumfahrt (DLR)
51170 Köln, Germany
Tel.: +49 2203 601 4582
Fax: +49 2203 601 2255
E-mail: peter.galenko@dlr.de

You will find the article and additional material by entering the document number **MK110297** on our website at *www.ijmr.de*

Appendix

A. Free energy density for a dilute system

A dilute alloy approximation has been previously used in the phase-field model adopted for the problem of solute trapping [14]. Following this advancement, we give details of derivation for the contributions from atoms to the free energy density in the dilute system approximation. Using approximation of an ideal solution of A and B atoms, the free energy density in a bulk liquid is

$$f_{\mathrm{L}}(c_{\mathrm{A}}, c_{\mathrm{B}}, T) = \frac{RT}{v_{\mathrm{m}}}(c_{\mathrm{A}} \ln c_{\mathrm{A}} + c_{\mathrm{B}} \ln c_{\mathrm{B}}) \tag{29}$$

and the free energy density in a bulk solid is

$$f_{\mathrm{S}}(c_{\mathrm{A}}, c_{\mathrm{B}}, T) = \frac{RT}{v_{\mathrm{m}}}(c_{\mathrm{A}} \ln c_{\mathrm{A}} + c_{\mathrm{B}} \ln c_{\mathrm{B}})$$
$$+ \frac{RT}{v_{\mathrm{m}}}(c_{\mathrm{A}} F_{\mathrm{A}}(T) + c_{\mathrm{B}} F_{\mathrm{B}}(T)) \tag{30}$$

where v_{m} is the molar volume taken to be the same in both phases and F_{A} and F_{B} describe contributions from atoms of A-sort and B-sort, respectively. Taking Eqs. (29) and (30) into account, one can define chemical potentials for both phases as

$$\mu_{\mathrm{A}}^{\mathrm{L}} = \frac{\partial f_{\mathrm{L}}}{\partial c_{\mathrm{A}}} = \frac{RT}{v_{\mathrm{m}}}(1 + \ln c_{\mathrm{A}})$$

$$\mu_{\mathrm{A}}^{\mathrm{S}} = \frac{\partial f_{\mathrm{S}}}{\partial c_{\mathrm{A}}} = \frac{RT}{v_{\mathrm{m}}}(1 + \ln c_{\mathrm{A}}) + \frac{RT}{v_{\mathrm{m}}} F_{\mathrm{A}}(T) \tag{31}$$

$$\mu_{\mathrm{B}}^{\mathrm{L}} = \frac{\partial f_{\mathrm{L}}}{\partial c_{\mathrm{B}}} = \frac{RT}{v_{\mathrm{m}}}(1 + \ln c_{\mathrm{B}})$$

$$\mu_{\mathrm{B}}^{\mathrm{S}} = \frac{\partial f_{\mathrm{S}}}{\partial c_{\mathrm{B}}} = \frac{RT}{v_{\mathrm{m}}}(1 + \ln c_{\mathrm{B}}) + \frac{RT}{v_{\mathrm{m}}} F_{\mathrm{B}}(T) \tag{32}$$

Phase diagram for equilibrium coexistence of phases is defined by the equality of chemical potentials:

$$\mu_{\mathrm{A}}^{\mathrm{L}} = \mu_{\mathrm{A}}^{\mathrm{S}}, \quad \mu_{\mathrm{B}}^{\mathrm{L}} = \mu_{\mathrm{B}}^{\mathrm{S}} \tag{33}$$

In equilibrium, the condition (33) and definitions (31) and (32) give

$$1 + \ln c_{\mathrm{A}}^{\mathrm{L}} = 1 + \ln c_{\mathrm{A}}^{\mathrm{S}} + F_{\mathrm{A}}(T) \tag{34}$$

$$1 + \ln c_{\mathrm{B}}^{\mathrm{L}} = 1 + \ln c_{\mathrm{B}}^{\mathrm{S}} + F_{\mathrm{B}}(T) \tag{35}$$

Assuming A-atoms as solvent and B-atoms as a solute, then from Eq. (35) and definition of equilibrium partition coefficient

$$k_{\mathrm{e}} = \frac{c_{\mathrm{S}}}{c_{\mathrm{L}}} \tag{36}$$

the contribution $F_{\mathrm{B}}(T)$ to the free energy from B-atoms is obtained as follows

$$\ln \frac{c_{\mathrm{B}}^{\mathrm{S}}}{c_{\mathrm{B}}^{\mathrm{L}}} = -F_{\mathrm{B}}(T), \quad F_{\mathrm{B}} = -\ln k_{\mathrm{e}} \tag{37}$$

Using the total mass balance $c_{\mathrm{A}} + c_{\mathrm{B}} = 1$, from Eqs. (34) and (36) one gets

$$F_{\mathrm{A}}(T) = \ln \frac{c_{\mathrm{A}}^{\mathrm{L}}}{c_{\mathrm{A}}^{\mathrm{S}}} = \ln \frac{1 - c_{\mathrm{B}}^{\mathrm{L}}}{1 - k_{\mathrm{e}} c_{\mathrm{B}}^{\mathrm{L}}} \tag{38}$$

Assuming the straight line for the liquidus $T_{\mathrm{L}} = T_{\mathrm{A}} + m_{\mathrm{e}} c_{\mathrm{B}}^{\mathrm{L}}$, one can find equilibrium connection between concentration and temperature as $c_{\mathrm{B}}^{\mathrm{L}} = -(1/m_{\mathrm{e}})(T_{\mathrm{A}} - T)$. Substituting the latter expression into Eq. (38), finally, we obtain the contribution $F_{\mathrm{A}}(T)$ to the free energy from A-atoms:

$$F_{\mathrm{A}}(T) = \ln \frac{1 + (1/m_{\mathrm{e}})(T_{\mathrm{A}} - T)}{1 + (k_{\mathrm{e}}/m_{\mathrm{e}})(T_{\mathrm{A}} - T)} \tag{39}$$

The present derivation for contributions (37) and (39) can be merely extended to the cases of non-ideal solutions.